



Sharif University of Technology
Scientia Iranica
Transactions B: Mechanical Engineering
www.scientiairanica.com



Novel method for performance degradation assessment and prediction of hydraulic servo system

Zh. Wang, Ch. Lu, J. Ma*, H. Yuan and Z. Chen

Science & Technology on Reliability & Environmental Engineering Laboratory, School of Reliability and Systems Engineering, Beijing, China.

Received 22 May 2014; received in revised form 20 January 2015; accepted 14 April 2015

KEYWORDS

Hydraulic servo system;
Performance degradation assessment;
Mean impact value;
Mahalanobis distance;
Elman neural network.

Abstract. Performance degradation assessment and prediction of hydraulic servo systems has attracted increasing attention in recent years. This study proposes a performance degradation assessment and prediction method based on Mean Impact Value (MIV), Mahalanobis Distance (MD), and Elman neural network. First, a state observer based on Radial Basis Function (RBF) is designed to calculate the residual error between the actual and estimated outputs, and typical time-domain features, such as Root Mean Square (RMS), peak value and kurtosis, are extracted. Second, the MIV analysis based on BP neural network is applied to evaluate the sensitivity of each extracted feature, and the selected optimal features are employed to construct the Mahalanobis space for normal states. Third, the MD between the most recent state and the constructed space of normal state is calculated, which can be normalized into a confidence value so as to assess the performance. Finally, an Elman neural network is used to predict the degradation trend. The proposed method is proven to be effective by a simulation model with the commonly occurring faults.

© 2015 Sharif University of Technology. All rights reserved.

1. Introduction

Hydraulic servo systems have become widely used in automatic control and power transmission systems due to their advantages on large driving force and rapid responses. As a subsystem, hydraulic servo system has a great impact on the functionality and efficiency of complex primary system, failure of which may result in serious economic losses, therefore, it is of great importance to make sure the system works in the normal state in order that maintenance actions should be carried out timely. Thus, Condition-Based Maintenance (CBM) based on performance degradation assessment and prediction has received more attention,

which can be performed once performance degradation occurs [1].

A variety of hydraulic servo system performance degradation assessments and prediction researches have been conducted. These studies mainly focus on four aspects: signal analysis, cluster analysis, health indicators prediction, and pattern recognition. Recently, two-stage neural network and FARX model methods have been proposed for fault detection and location [2,3], but these methods do not involve performance assessment and prediction of system degradation, which is insufficient to support the CBM. A review of advanced time-frequency analysis methods for machinery fault diagnosis is carried out by Feng [4], and some performance assessment methods for typical mechanical components such as bearings and gearboxes are proposed [5], however, the signals of such components are rapidly varying, which means

*. Corresponding author. Tel.: 0086-10-82339346;
Fax: 0086-10-82314746
E-mail address: majian3129@126.com (J. Ma)

the methods for typical mechanical components may be unsuitable for hydraulic servo systems. To improve veracity and reliability, some methods are proposed to select the best fit features. An approach based on support vector regression model and Mean Impact Value (MIV) is proposed for active compounds identification, which can realize feature optimization effectively [6]. Currently, the performance of hydraulic servo systems is always assessed by calculating the overlap or distance between the real-time features and the baseline features in the feature space, such as SOM and GMM. A fault observer and SOM neural network-based assessment method has been proposed [7], but the amount of SOM data as a neural network is rather large, and the extracted residual information is insufficient to assess the hydraulic servo system since RMS is the only indicator extracted from residuals. Mahalanobis Distance (MD), proposed by Mahalanobis in 1936, is an effective method that can identify and measure the similarity of an unknown sample set to a known one [8]. In this research, it is used to propose a new method for performance assessment of hydraulic servo system. The performance degradation of hydraulic servo systems is always predicted by the neural network. A simulation study based on artificial neural network is introduced for nonlinear time-series forecasting by Zhang [9], and a normalized RBF neural network is applied to predict the trend of chaotic signals [10]. However, the convergence rate of prediction is rather slow, while the amount of training data is rather huge. Elman neural network is a kind of dynamic neural network, which shows good calculation rate and precision in performance prediction via dynamic historical data [11].

To solve the aforementioned problems, a method that incorporates MIV, MD and Elman neural network is proposed in this paper. The remainder is organized as follows. Section 2 introduces the material and methods of performance degradation assessment and prediction. Section 3 discusses the results of the simulation experiment. Section 4 concludes the work.

2. Material and methods

Figure 1 is a flowchart of the method for performance degradation assessment and prediction of hydraulic servo systems based on RBF state observer, MIV, MD and Elman neural network. The method consists of four parts: condition monitoring, feature extraction/optimization, performance assessment, and performance degradation prediction. First, a state observer model based on RBF neural network is used to estimate the output of a real system, then residual error between the system output and the output estimated

by the observer is obtained, which turns to be a considerable difference in magnitude between normal and fault states. Second, typical time-domain features are extracted from the residual errors of different states, and MIV of each feature is calculated based on BP neural network so as to reduce the redundancy features. Third, the Mahalanobis space is constructed by multi-dimensional points, coordinate values of which are the selected features, then the MD and CV are calculated to assess the performance. Finally, an Elman neural network is used to predict the future CV via dynamic historical data.

2.1. Condition monitoring with a state observer model based on RBF neural network

Hydraulic servo system is a kind of non-linear complex system, which is difficult to be defined using mathematical expression. Compared with linear methods, nonlinear methods such as neural network show better sensitivity to fault states of hydraulic servo systems. The state observer based on neural network can approximate the real system well with enough input and output neurons. In this study, an RBF neural network is used because of the nonlinear mapping capability and training efficiency.

2.1.1. Structure of RBF network

In the field of mathematical modeling, a radial basis function network is an artificial neural network that uses radial basis functions as activation functions, which can be applied to multiple fields [12]. The RBF neural network consists of three layers: input layer, hidden layer and output layer (see Figure 2); the input and hidden layers are non-linear mapping relationship. The output of the network is a linear combination of radial basis functions of the inputs and neuron parameters. Normally, a Gaussian function is chosen as the radial basis function. Suppose x and y are the input and output vectors, and the output of the hidden layer can be described as:

$$u_i = \exp \left[\frac{(x - c_i)^T (x - c_i)}{2\sigma_i^2} \right] \quad (i = 1, 2, 3 \cdots q), \quad (1)$$

where μ_i , σ_i , q , and c_i denote the output, standard constant, quantity of hidden layer nodes, and Gaussian function central vector, respectively. σ_i and c_i can be determined by the sample input.

Linear mapping between the hidden layer and output layer is defined as:

$$y_k = \sum_{i=1}^q \omega_{ki} u_i - b_k \quad (k = 1, 2, \cdots, L), \quad (2)$$

where ω_{ki} and b_k denote the weighting coefficient and threshold of the output layer, respectively.

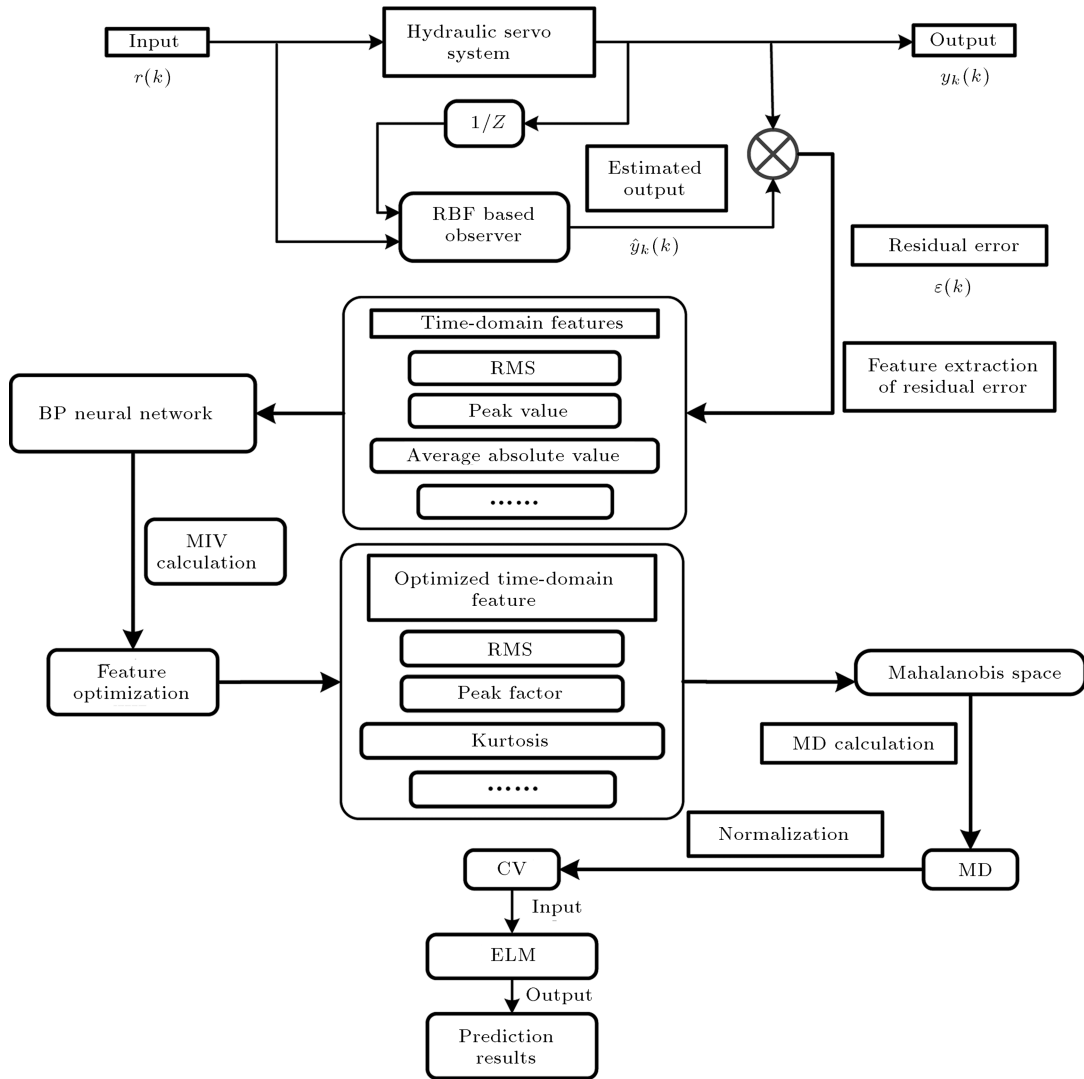


Figure 1. Flowchart for the proposed performance degradation assessment and prediction method.

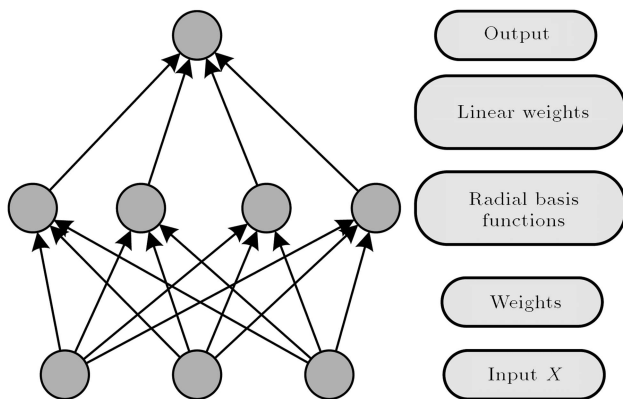


Figure 2. Structure of RBF network.

2.1.2. Residual error calculation

A state observer model can be established based on the trained RBF neural network. The residual error is generated based on a comparison between the actual and the estimated system response.

Suppose that the hydraulic servo system can be described as:

$$\begin{cases} X(t) = g(t, X, U, Y, f) \\ Y(t) = g(t, X, U, Y, f) \end{cases} \quad (3)$$

Then the state observer is defined as:

$$\begin{cases} \hat{X}(t) = g(t, \hat{X}, U, \hat{Y}, f) \\ \hat{Y}(t) = g(t, \hat{X}, U, \hat{Y}, f) \end{cases} \quad (4)$$

Suppose $X(t)$, $Y(t)$, $U(t)$ and $f(t)$ are the input vectors, output vectors, state vectors, and failure vectors of actual hydraulic servo systems, respectively, then the inputs of RBF neural networks are set as $X(t)$ and $Y(t-1)$ (see Figure 1), and the estimated output is $\hat{Y}(t)$.

The residual error is defined as the difference between the actual and estimated outputs:

$$e(t) = Y(t) - \hat{Y}(t). \quad (5)$$

If $\lim_{t \rightarrow \infty} e(t) = 0$ when $f(t) = 0$ or $f(t) \neq 0$, the RBF observer model turns to be effective [13].

2.2. Performance assessment based on MIV-MD

Variety of time-domain features can be extracted from the residual error, such as Root-Mean-Square (RMS), peak, kurtosis, etc. The features can reflect the normal and fault states of hydraulic servo systems accurately. Suppose P_1, P_2, \dots, P_i represent the typical time-domain features vectors. If there are N points in the residual error sequence, $n(n = \frac{N}{M})$ feature points will be extracted from M points ($M \leq N$) to generate Mahalanobis space.

However, the fault features are not all sensitive to the fault state of hydraulic servo systems, which means there may exist useless features in the performance assessment and prediction. Moreover, in consequence of the redundancy features, the calculation process of MD is much more complex in the multi-dimensional space, while the result of assessment is not much better than that in the low-dimensional space. To solve this problem, mean impact value is introduced in the study to obtain the optimal feature.

2.2.1. Feature optimization based on MIV

Mean impact value is deemed to be a good index that can be applied to evaluate the relationship of variables in the neural network, especially reflecting the influence degree between input variables and output variables. Plus-minus and absolute value of the MIV are related to the correlation direction and influence degree, respectively [14].

The MIV based on BP neural network is calculated as follows:

1. Train the BP neural network with an original sample set S , and predict the regression;
2. Add and subtract 10 percent of each variable in S to generate two new sample sets S_1 and S_2 ;
3. Set S_1 and S_2 as inputs to perform the simulation based on the trained BP neural network, and the results are defined as M_i and D_i ;
4. W_i Indicated the degree of influence each independent variable has on the output variable, which can be calculated as:

$$W_i = M_i - D_i. \quad (6)$$

5. Finally, calculate the MIV as:

$$\text{MIV} = \frac{W_1 + W_2 + \dots + W_N}{N}, \quad (7)$$

where N indicates the test times.

The MIVs can be sorted in descending order based on absolute values, where the top independent variables

have larger influence on the output in the BP neural network. In this study, time-domain features are set as the input variables, while the output is a numerical value representing the fault state, then the best fit features can be selected via the proposed method.

2.2.2. MD calculation and its normalization

The MD is a measure of the distance between a point P and a distribution R , which is a multi-dimensional generalization of the idea of measuring how many standard deviations away P is from the mean of R . This distance grows as P moves away. In the study, suppose:

$$C_1(\alpha_{01}, \dots, \gamma_{01}), C_2(\alpha_{02}, \dots, \gamma_{02}), \dots, C_n(\alpha_{0n}, \dots, \gamma_{0n}),$$

are the optimized feature points in normal state, then a reference space R is denoted by $\{C_1, C_2, \dots, C_n\}$. Suppose:

$$X_1(\alpha_1, \dots, \gamma_1), X_2(\alpha_2, \dots, \gamma_2), \dots, X_n(\alpha_n, \dots, \gamma_n)$$

are the feature points that belong to different fault states. The MD d_1, d_2, \dots, d_n will be calculated by the proposed method, which is used to assess the performance of hydraulic servo systems. It only needs one feature point once the Markov space is built.

The flowchart of the MD calculation process is shown in Figure 3.

The MD is calculated as:

$$\text{MD}_j = \frac{1}{k} Z_{ij}^T C^{-1} Z_{ij}, \quad (8)$$

where C and Z_{ij} indicate the correlation matrix and the column vector of standardized variables, respectively. MD_j is the MD for the j th observation [15]. The MDs obtained from normal states are closer to the constructed Mahalanobis space, compared with those obtained from performance degradation or fault states.

To display the assessment results intuitively, Confidence Value (CV) is adopted in the paper proposed by Qiu to normalize the MD into $[0, 1]$ [16], which can be formulated as below:

$$\text{CV}_i = 1 - \frac{\arctan(d_i + \alpha) - \arctan(\alpha)}{\pi/2 - \arctan(\alpha)}, \quad (9)$$

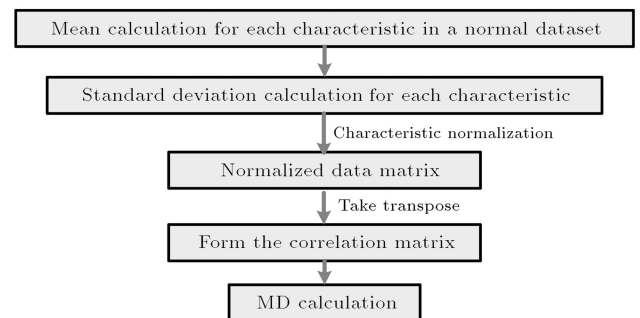


Figure 3. Process of MD calculation.

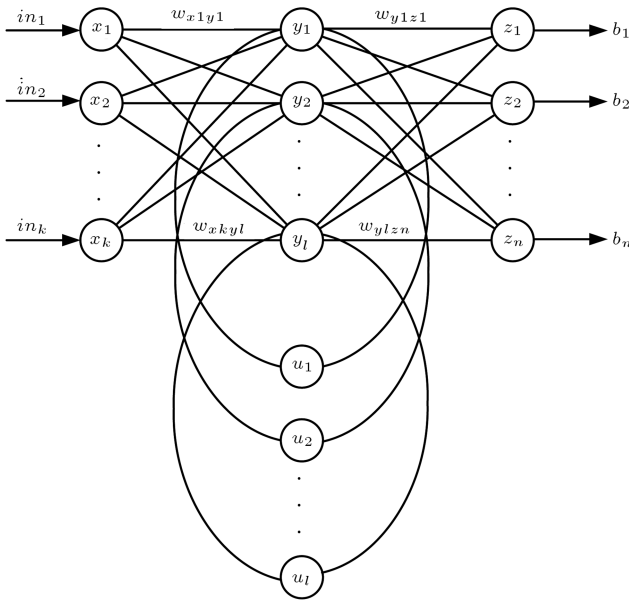


Figure 4. Structure of Elman neural network.

where d_i and α indicate the MD and a shape parameter. The CV varies with the MD synchronously and oppositely, and it will be larger as the system shows better performance.

2.3. Performance trend prediction based on Elman neural network

2.3.1. Structure of Elman neural network

Elman neural networks work for the generalized single-hidden layer feed-forward networks, which consist of four layers: input layer, hidden layer, acceptor layer and output layer, which are arranged vertically as x, y and z in Figure 4, with the addition of a set of “context units” (u in Figure 4). There are connections from the middle (hidden) layer to these context units fixed with a weight of one. At each time step, the input is propagated in a standard feed-forward fashion, and then a learning rule is applied. The fixed back connections result in the context units always maintaining a copy of the previous values of the hidden units. Thus, the Elman neural network can maintain a sort of state, allowing it to perform the tasks such as sequence-prediction that are beyond the power of a standard multilayer perceptron.

Mathematical model of the Elman neural network is described as below.

$$x(k) = f(\omega_{I1}x_C(k) + \omega_{I2}\mu(k-1)), \quad (10)$$

$$x_C(k) = \alpha x_C(k-1) + x(k-1), \quad (11)$$

$$y(k) = g(\omega_{I3}x(k)), \quad (12)$$

where ω_{I1} , ω_{I2} and ω_{I3} indicate the weight matrices of acceptor layer/input layer, input layer/hidden layer, and hidden layer/output layer, respectively. $x(k)$ and

$x_C(k)$ are the outputs of acceptor and hidden layers, while $y(k)$ is the output of output layer. $\alpha \in [0, 1]$ indicates the gain factor, and $f(x)$ is commonly defined as sigmoid function, which is formulated as:

$$f(x) = \frac{1}{1 + e^{-x}}. \quad (13)$$

2.3.2. Learning process of Elman neural network

Suppose actual output is $y_d(k)$ in the k th simulation node; the objective function $E(k)$ is defined as:

$$E(k) = \frac{1}{2}(y_d(k) - y(k))^T(y_d(k) - y(k)). \quad (14)$$

Partial derivatives for each weight can be calculated based on gradient descent method, then the learning algorithm is obtained if the value of partial derivative is 0.

$$\omega_{I3}^{ij} = \eta_3 \delta_i^0 x_j(k) \quad (i = 1, 2, \dots, m; j = 1, 2, \dots, n), \quad (15)$$

$$\omega_{I2}^{jq} = \eta_2 \delta_j^h \mu_q(k-1) \quad (j = 1, 2, \dots, n; q = 1, 2, \dots, r), \quad (16)$$

$$\omega_{I1}^{jl} = \eta_1 \sum_{i=1}^m (\delta_i^0 \omega_{I3}^{ij}) \frac{\partial x_j(k)}{\omega_{I1}^{jl}} \quad (j = 1, 2, \dots, n; l = 1, 2, \dots, n) \quad (17)$$

$$\delta_i^0 = (y_{d,i}(k) - y_i(k))g'_i(\cdot), \quad (18)$$

$$\delta_j^h = \sum_{i=1}^m (\delta_i^0 \omega_{I3}^{ij}) f'_j(\cdot), \quad (19)$$

$$\frac{\partial x_j(k)}{\partial \omega_{I1}^{jl}} = f'_j(\cdot) x_l(k-1) + \alpha \frac{\partial x_j(k-1)}{\partial \omega_{I1}^{jl}} \quad (j = 1, 2, \dots, n; l = 1, 2, \dots, n), \quad (20)$$

where η_1 , η_2 and η_3 indicate the learning steps of the weights.

The characteristic of Elman neural network is that the input and output of hidden layer connect with each other because of the delay and storage of acceptor layer, and the inside feedback network also increases the ability of dynamic information processing to serve the purpose of dynamic modeling [17]. With these characteristics, Elman neural network can be applied to predict the CV via historical data. The manner of the prediction process is like a sliding window, using the last $N(N \geq 1)$ values to predict the future $M(M \geq 1)$ values continuously, and the prediction accuracy is higher as the historical data increases.

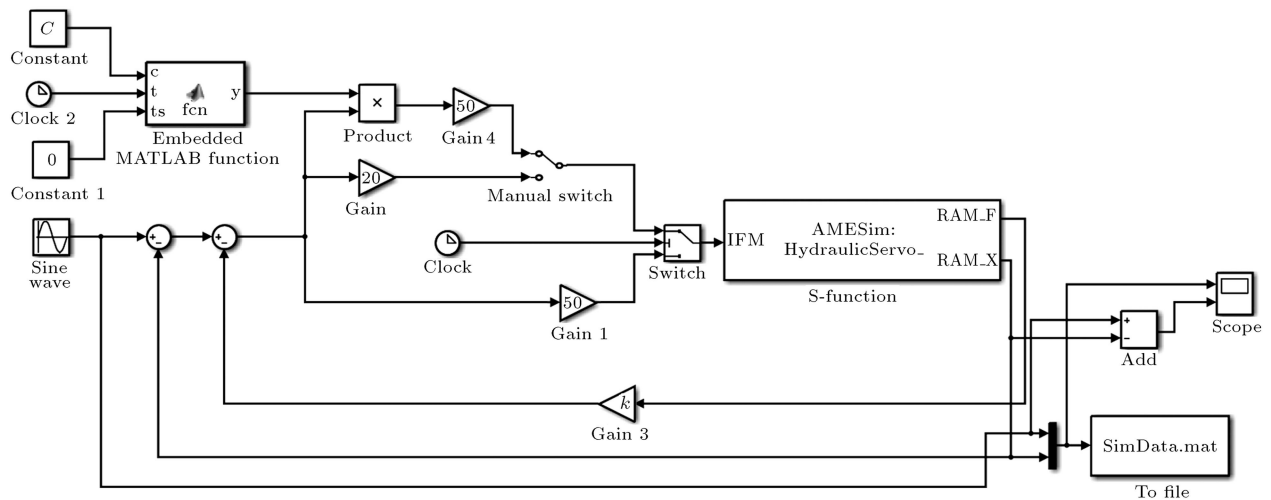


Figure 5. Simulation model of hydraulic servo system.

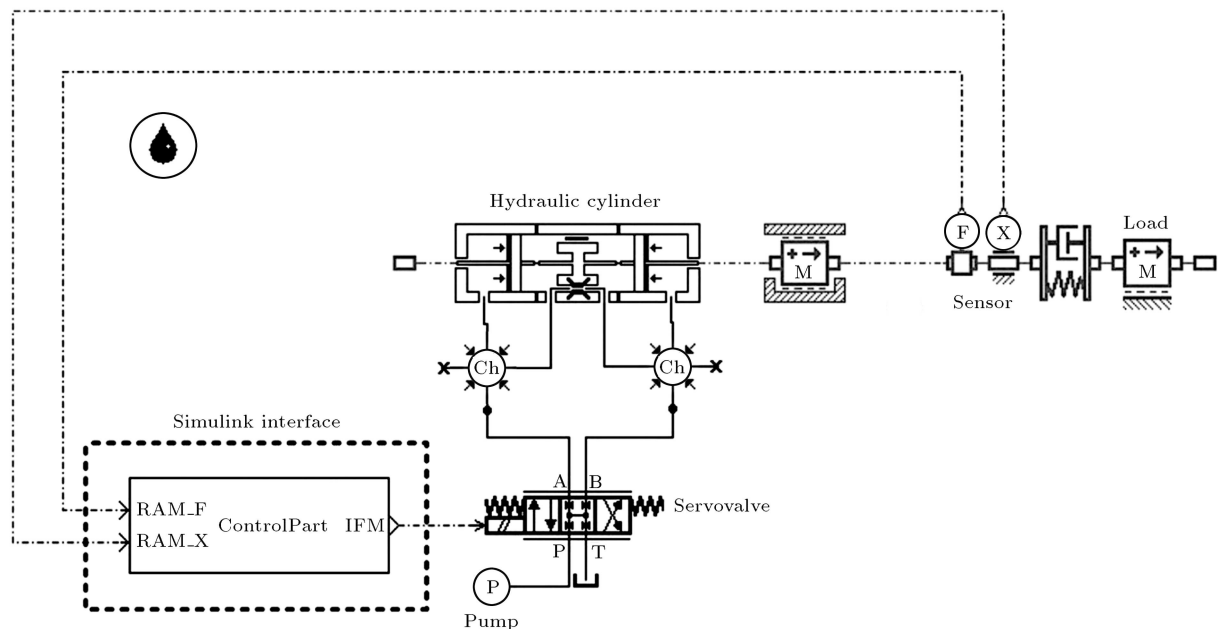


Figure 6. Mechanical part in AMESim.

3. Experimental results

Two experiments were conducted to illustrate the effectiveness of the presented method, and the data used in the experiments is based on combined-simulation of AMESim and Matlab. The first experiment is used to validate the effectiveness of performance assessment method for hydraulic servo systems, while the other experiment focuses on the validation of performance degradation trend prediction.

3.1. Experiment 1: performance assessment of hydraulic servo system

Statistical data indicates that the typical fault states of the systems are electronic amplifier faults, leakage faults, sensor faults, etc. In this study, internal leakage

fault and electronic amplifier fault were injected to demonstrate the proposed method, which represented abrupt fault state and gradual fault state, respectively. The details of experiment processes are described below.

The simulation model of the hydraulic servo system was established by Matlab Simulink and AMESim. Figure 5 showed the control part, which was established in Simulink environment; the mechanical part was shown in Figure 6, which was converted to a Simulink S-Function to be imported to Simulink.

The physical parameters of the servo valve are shown in Table 1.

Considering the injection of leakage faults, the cylinder module contained three sub-modules: two piston modules and one leakage module.

Table 1. Physical parameters of the servo valve.

	Ports parameters			
	<i>P</i> to <i>A</i>	<i>P</i> to <i>B</i>	<i>B</i> to <i>T</i>	<i>A</i> to <i>T</i>
Flow of maximum open valve	80 L/min	80 L/min	80 L/min	80 L/min
Pressure drop	100 bar	100 bar	100 bar	100 bar
Critical flow number	1000	1000	1000	1000
Valve parameters				
Rated current	1.5 mA			
Natural frequency	500 Hz			
Fraction dead band	0			
Damping ratio	0.7			
Working density of fluid	880 kg/m ³			
Kinematic viscosity	60 cSt			

Table 2. Physical parameters of cylinder module.

Piston module parameters	
External piston diameter	90 mm
Chamber length (0 displacement)	150 mm
Rod diameter	30 mm
Damping ratio	0.7
Leakage module parameters	
Diameter clearance	1e-05 mm
Contact length	30 mm

Table 3. Parameters of electronic amplifier (normal and fault).

State	Gain (<i>Kv</i>)
Normal	50
Fault	30

The physical parameters of the sub- modules are shown in Table 2.

Thus, the parameters of the simulation model were set, and the details of fault injection are described below:

1. Electronic amplifier fault injection: Electronic amplifier fault injection module is shown in Figure 4, which is conducted in Simulink environment. The parameters of normal amplifier and fault amplifier are shown in Table 3.
2. Leakage fault injection: To compare the performance assessment results under different degradation levels, slight leakage, fault, moderate leakage fault and severe leakage fault were injected. The physical parameters of leakage faults are shown in Table 4.

3.1.1. Features extraction

A simulation model with fault injection modules was presented to evaluate the proposed method (see Figures 4 and 5).

Table 4. Physical parameters of leakage faults.

Clearance on diameter	Value
Slight leakage fault	0.9 mm
Moderate leakage fault	1.0 mm
Severe leakage fault	1.1 mm

The input signal for the simulation model of leakage fault injection was:

$$r(t) = 0.12 \sin \pi t. \quad (21)$$

The input signal for the simulation model of amplifier fault injection was:

$$r(t) = 0.1 \sin \frac{\pi}{4} t. \quad (22)$$

The transfer function of the amplifier was:

$$f(t) = c_0 K_v; \quad (c_0 = 1). \quad (23)$$

The gradual fault injection function was:

$$f(t) = \exp[c_2(t - t_s)](c_2 = 0.05; t_s = 30). \quad (24)$$

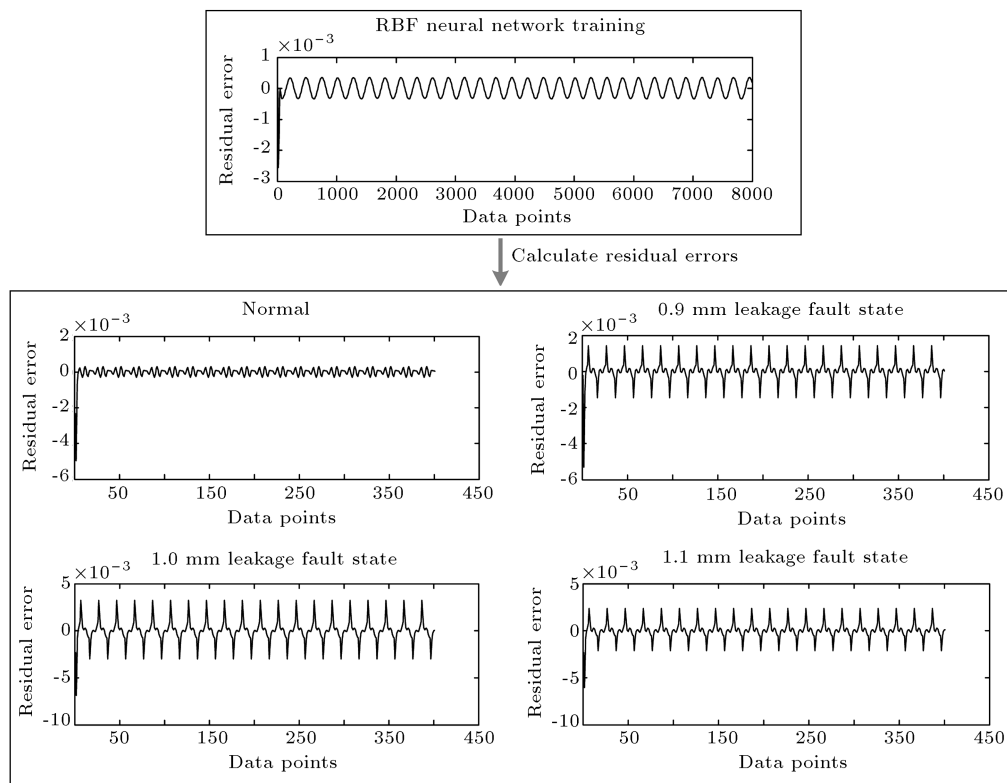
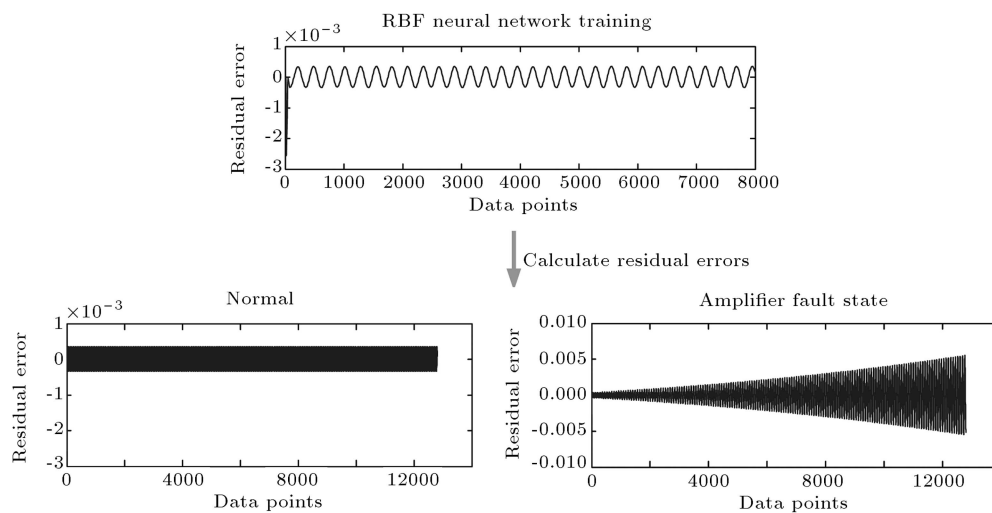
The details of each test are shown in Table 5.

Residual errors of the hydraulic servo system in different states were calculated using the state observer trained by simulation data. The results are shown in Figures 7 and 8.

When the leakage fault was injected, the sampling frequency was set 10 Hz, and the simulation time was 160 s with 1600 data points acquired. Among these points, each block of 20 data points was regarded as one cycle to extract the time-domain features. Residual errors of different leakage levels were successively obtained using the state observer, and the severe leakage showed the biggest residual values, which denoted the worst working condition.

Table 5. Details of each test.

	Fault mode	Fault injection time		
		Time	Raw data	One cycle data
Test 1	Normal (leakage)	40	400	20
Test 2	Normal (amplifier)	1280	12800	80
Test 3	Leakage fault clearance 0.9 mm	40	400	20
	Leakage fault clearance 1.0 mm	40	400	20
	Leakage fault clearance 1.1 mm	40	400	20
Test 4	Amplifier fault	1280	12800	80

**Figure 7.** Residual errors of leakage fault state.**Figure 8.** Residual errors of amplifier fault state.

For the amplifier fault injection, the sampling frequency remained the same as that of the leakage fault. The simulation time was modified as 1280 s for sufficient experimental data. The time-domain features were extracted every other 80 points. Residual errors ascended to about 0.005 from 0 in 1280s, which denoted the working condition was degrading.

3.1.2. Features optimization based on MIV analysis

To comprehensively represent the characteristic of residual errors, 10 time-domain features were extracted, such as mean absolute value, RMS, kurtosis, variance, peak, shape factor, etc. Then the MIV was used to realize feature optimization. In this study, leakage and amplifier faults were employed for validation.

MIVs are usually calculated based on BP neural network. The input variables of the BP network were the 10 normalized time-domain features, and the output was a numerical value representing different fault states, which is assigned 0, 1, and 2 for the normal state, leakage fault state, and amplifier fault state, respectively. The hidden layer nodes were calculated as:

$$k = \sqrt{a + b} + c, \quad (25)$$

where $c \in [1, 10]$; a and b represent the input and output neurons, respectively. The BP neural network exhibited good convergence when $k = 13$. To determine the suitable training time, the learning speed was set as 0.1, and the expectant error was 0.005.

After RBF neural network was trained, MIVs of different features were calculated based on the proposed method. The results are listed in Table 6.

Figure 9 shows a visualized comparison of the extracted features, where the area of fans indicates the influence degree of each time-domain feature. In Figure 9(a), we could notice that MIVs of kurtosis, peak, RMS, peak factor and margin factor were the top five when leakage fault was injected, while in the amplifier fault state the top five were RMS, mean value, kurtosis, peak factor and peak on the right

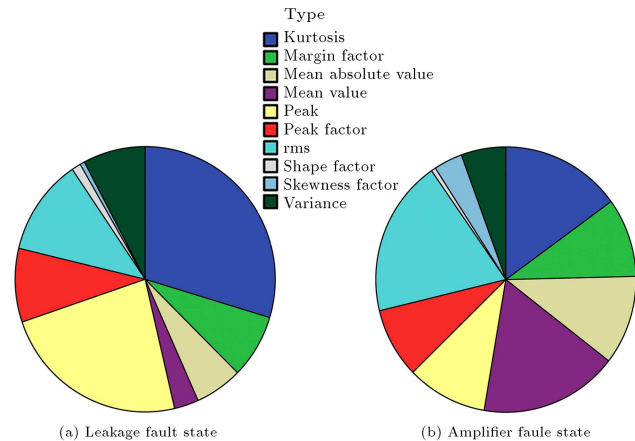


Figure 9. Influence degree of each time-domain feature on the leakage and amplifier fault states.

figure. Among them, RMS, peak factor, and kurtosis were sensitive to both abrupt and gradual fault states, which means the three features were the best fit for performance assessment of the hydraulic servo system in the study.

3.1.3. Performance assessment using the MD

The Mahalanobis space could be constructed by the three-dimensional feature points, coordinates of which were determined by RMS, peak factor and kurtosis values, then the MDs of the two fault states were calculated. The state of initial 40 s indicated the normal state for the leakage fault injection, and 0.9 mm/1.0 mm/1.1 mm leakage fault was injected after every other 40 s. For the amplifier fault injection, the value of Kv was decreased to 20 from 50 in 1280 s. The results are shown in Figure 10.

From Figure 10, we can see that the values of MD were increased with the injected leakage and amplifier faults, while the CVs were decreased synchronously, and there was a considerable difference in the magnitude between the normal and fault states. On Figure 10(a), the CV appears to be a stepped decrease when the internal leakage faults with clearance diameters of 0.9/1.0/1.1 mm were injected, and the

Table 6. MIVs of time-domain features.

Mean impact value					
Leakage fault mode	Average absolute value	Mean value	Peak factor	RMS	Kurtosis
	0.2127	-0.1088	0.3236	0.4239	-1.0683
	Variance	Skewness factor	Shape factor	Margin factor	Peak
	0.2793	0.0206	0.0413	0.2801	0.8433
Amplifier fault mode	Average absolute value	Mean value	Peak factor	RMS	Kurtosis
	0.4127	0.6512	-0.4496	0.7239	0.5683
	Variance	Skewness factor	Shape factor	Margin factor	Peak
	-0.2110	0.1347	-0.0213	0.3646	0.3793

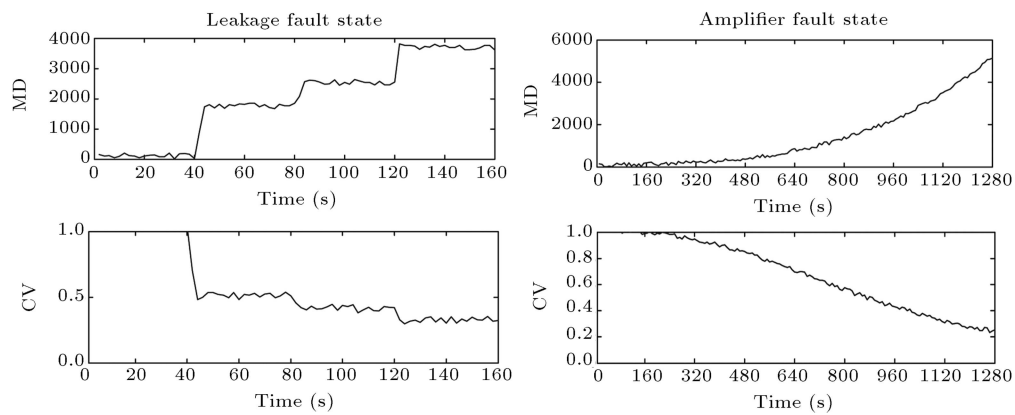


Figure 10. Performance assessment of the hydraulic servo system.

CV on Figure 10(b) declined continuously along with the variation of Kv . These results indicate that the proposed method is an effective method to perform performance assessment of hydraulic servo systems, which can not only detect the occurrence of both abrupt faults and gradual faults, but also reflect the degradation in performance.

3.2. Experiment 2: Performance trend prediction

The amplifier gradual confidence value could be an effective index for determining the time when maintenance should be carried out. To realize performance trend prediction via the truncated data, Elman neural network was trained to predict the CVs. The hidden layer nodes were 7, and training steps were set to 1000. Considering precision and synchronization of the prediction, the width of the slide window is 400. To demonstrate the excellent learning ability, the Elman neural network was trained by initial 3200, 4800, and 6400 points, respectively, then the last CVs were predicted, as shown in Figure 11.

In Figure 11, the black curve represented the actual CV obtained by the MD method, while the blue, green and amaranth curves were the CVs predicted by the Elman neural network, which were trained by different amounts of historical data. In this study,

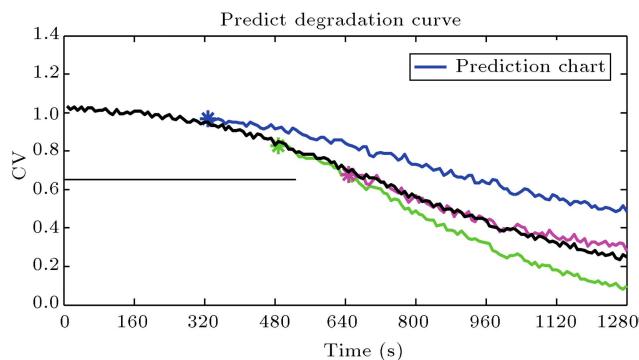


Figure 11. Performance prediction of the hydraulic servo system.

Table 7. Details of Performance trend prediction experiment.

Curse	Trained time		Result	
	Time	Raw data epoch	CV at 1280 s	Prediction deviation
Black	1280	12800	0.249	0
Blue	320	3200	0.485	-0.236
Green	480	4800	0.097	0.152
Amaranth	640	6400	0.281	-0.032

the trained time of 320 s, 480 s, and 640 s were applied, respectively. Details of the performance trend prediction experiment are shown in Table 7.

The results showed that the prediction error of Elman neural network decreased with longer training time, which demonstrated the effect of the approach for the truncated data prediction. When the training time was 640 s, the prediction deviation of CV was -0.032, which showed very high accuracy.

4. Conclusion

This paper proposes a method for performance degradation assessment and prediction of hydraulic servo systems based on MIV, MD and Elman neural network. The advantage of the work lies in the efficient synergy of each method. Time-domain features are extracted from the residual error to construct the Mahalanobis space, then MD is calculated to assess the performance. Moreover, MIV based on BP neural network is introduced to select the optimal features, which reduces the dimension of feature vectors, thus strengthening the MD calculation process. Finally, Elman neural network is applied to performance degradation prediction. Two experiments are presented to demonstrate the effectiveness and feasibility of the proposed method.

Acknowledgments

This research was supported by the National Natural Science Foundation of China (Grant No. 61074083 and

51105019), and by the Technology Foundation Program of National Defense (Grant No. Z132013B002).

References

1. Lee, J. "Machine performance monitoring and proactive maintenance in computer-integrated manufacturing: Review and perspective", *International Journal of Computer Integrated Manufacturing*, **8**(5), pp. 370-380 (1995).
2. He, X. "Fault diagnosis approach of hydraulic system using FARX model", *Procedia Engineering*, **15**(0), pp. 949-953 (2011).
3. Liu, H., Wang, S. and Ouyang P. "Fault diagnosis in a hydraulic position servo system using RBF neural network", *Chinese Journal of Aeronautics*, **19**(4), pp. 346-353 (2006).
4. Feng, Z., Liang, M. and Chu, F. "Recent advances in time-frequency analysis methods for machinery fault diagnosis: A review with application examples", *Mechanical Systems and Signal Processing*, **38**(1), pp. 165-205 (2013).
5. Pan, Y., Chen, J. and Guo, L. "Robust bearing performance degradation assessment method based on improved wavelet packet-support vector data description", *Mechanical Systems and Signal Processing*, **23**(3), pp. 669-681 (2009).
6. Chorowski, J., Wang, J. and Zurada, J.M. "Review and performance comparison of SVM- and ELM-based classifiers", *Neurocomputing*, **128**(1), pp. 507-516 (2014).
7. Liu, D., Liu, H., Tao, X. and Lu, Ch. "Research on performance degradation assessment for hydraulic servo system based on fault observer and SOM network", *Lecture Notes in Information Technology*, Hongkong: Information Engineering Research Institute, **14**(1), pp. 89-94 (2014).
8. De Maesschalck, R., Jouan-Rimbaud, D. and Massart, Désiré L. "The Mahalanobis distance", *Chemometrics and Intelligent Laboratory Systems*, **50**(1), pp. 1-18 (2000).
9. Zhang, G.P., Patuwo, B.E. and Hu, M.Y. "A simulation study of artificial neural networks for nonlinear time-series forecasting", *Computer & Operations Research*, **28**(4), pp. 381-396 (2001).
10. Cowper, M.R., Mulgrew, B. and Unsworth, C.P. "Non-linear prediction of chaotic signals using a normalized radial basis function network", *Signal Processing*, **82**(5), pp. 775-789 (2002).
11. Ding, Sh., Xu, X. and Nie, R. "Extreme learning machine and its applications", *Neural Computing & Applications*, **25**(1), pp. 3-4 (2014).
12. Qasem, S.N. and Shamsuddin, S.M. "Radial basis function network based on time variant multi-objective particle swarm optimization for medical diseases diagnosis", *Applied Soft Computing-ASC*, **11**(1), pp. 1427-1438 (2011).
13. Lu, Ch., Yuan, H., Tao, L. and Liu, H. "Performance assessment of hydraulic servo system based on bi-step neural network and autoregressive model", *Journal of Vibroengineering*, **9**(15), pp. 1546-1559 (2013).
14. Wen, G., Wen, Y. and Tan, J. "Fault diagnosis of ball screw based on MIV and RBF neural network", *Design and Research*, **1**, Chinese (2014).
15. Soylemezoglu, A., Jagannathan, S. and Saygin, C. "Mahalanobis Taguchi system (MTS) as a prognostics tool for rolling element bearing failures", *Journal of Manufacturing Science and Engineering*, **132**(5), pp. 0510141-05101412 (2010).
16. Lee, J., Wu, F., Zhao, W., Ghaffari, M., Liao, L. and Siegel, D. "Prognostic and health management design for rotary machine systems - reviews, methodology and applications", *Mechanical Systems and Signal Processing*, **42**(1), pp. 313-334 (2014).
17. Li, P., Li, Y., Xiong, Q., Chai, Y. and Zhang, Y. "Application of a hybrid quantized Elman neural network in short-term load forecasting", *International Journal of Electrical Power & Energy Systems*, **55**(1), pp. 749-759 (2014).

Biographies

Zhenya Wang received his BE in Mechanical Engineering from Zhengzhou University, Zhengzhou, China, in 2013. He is a PhD currently in School of Reliability and Systems Engineering from Beihang University, Beijing, China. His research interests include: fault diagnosis, prognosis and health management.

Chen Lu received his BE in Faculty of Electronic Information and Electrical Engineering from Dalian University of Technology, Dalian, China, in 1996. He also received his PhD in School of Energy and Power Engineering from Dalian University of Technology, Dalian, China, in 2002. His research interests include: prognosis and health management and performance degradation prediction.

Jian Ma received his BE in School of Automation Science and Electrical Engineering from Beihang University, Beijing, China, in 2009. He also received his MSc in School of Reliability and Systems Engineering from Beihang University, Beijing, China, in 2012. He is a PhD now in the same School. His research interests include: fault diagnosis, deep learning and pattern recognition.

Hang Yuan received his BE in School of Electrical

Engineering and Automation from Henan Polytechnic University, Jiaozuo, China, in 2007. He is a PhD now in School of Reliability and Systems Engineering from Beihang University, Beijing, China. His research interests include: fault diagnosis, and data mining.

Zihan Chen received his BE in School of Reliability and Systems Engineering from Beihang University, Beijing, China, in 2014. He is an MSc currently in the same School. His research interests include: fault diagnosis and health management.